Pharm Res (2014) 31:2166–2177
DOI 10.1007/s11095-014-1316-4

RESEARCH PAPER

A Model for Targeting Colon Carcinoma Cells Using Single-Chain Variable Fragments Anchored on Virus-Like Particles via Glycosyl Phosphatidylinositol Anchor

Vipin Kumar Deo • Megumi Yui • Md. Jahangir Alam • Masahito Yamazaki • Tatsuya Kato • Enoch Y. Park

Received: 28 June 2013 / Accepted: 28 January 2014 / Published online: 26 February 2014

ABSTRACT

Purpose VLPs displaying tumor targeting single-chain variable fragments (VLP-rscFvs) which targets tumor-associated glycoprotein-72 (TAG-72) marker protein have a potential for immunotherapy against colon carcinoma tumors. In this study, scFvs anchored on VLPs using glycosylphosphatidylinositol (GPI) were prepared to target colon carcinoma spheroids *in vitro*.

Methods VLPs-rscFvs were produced by co-injecting two types of *Bombyx mori* nucleopolyhedrovirus (BmNPV) bacmids, encoding RSV-gag and rscFvs cDNA into silkworm larvae. Large unilamellar vesicles (LUVs) of 100 nm in diameter were made using 1,2-dioleoyl-*sn*-glycero-3-phosphocholine (DOPC) and packaged with Sulforhodamine B (SRB). LUV-SRB was used to associate with VLP-rscFvs assisted by GP64 present on VLP-rscFvs to produce VLP-rscFv associated SRB (VLP-rscFvs-SRB) at pH 7.5.

Results The antigenicity of the purified VLPs-rScFvs was confirmed by enzyme-linked immunosorbent assay (ELISA) using TAG-72 as antigen. LUV-SRB made of DOPC was used to associate with 100 μg of VLP-rscFvs to produce VLP-rscFv-SRB. Specific delivery and penetration of SRB up to 100 μm into the spheroids shows the potential of the new model.

Conclusions The current study demonstrated the display, expression and purification of VLP-rscFvs efficiently. As a test model VLP-rscFv-SRB were prepared which can be used for immunotherapy. rscFvs provide the specificity needed to target tumors and VLPs serve as carrier transporting the dye to target.

KEY WORDS large unilamellar vesicle · silkworm expression system · single-chain variable fragment · tumor-associated glycoprotein-72 · virus-like particle

ABBREVIATIONS

BmNPV	*Bombyx mori* nucleopolyhedrovirus
CLSM	Confocal laser scanning microscope
DOPC	1,2-dioleoyl-*sn*-glycero-3-phosphocholine
ELISA	Enzyme-linked immunosorbent assay
gag	Group antigen protein
GPI	Glycosylphosphatidylinositol
LUVs	Large unilamellar vesicles
mAbs	Monoclonal antibodies
RSV	*Rous sarcoma* virus
scFvs	Single-chain variable fragments
SRB	Sulforhodamine B
TAG-72	Tumor associated glycoparticle-72
VLP-rscFvs	VLPs displaying tumor targeting scFVs
VLP-rscFv-SRB	VLP-rscFv packaged SRB
VLPs	Virus-like particles

INTRODUCTION

Virus like particles (VLPs) are macromolecular structures that are formed using capsid protein from virus which can self-fold

Electronic supplementary material The online version of this article (doi:10.1007/s11095-014-1316-4) contains supplementary material, which is available to authorized users.

V. K. Deo • T. Kato • E. Y. Park (✉)
Research Institute of Green Science and Technology, Shizuoka University
836 Ohya, Suruga-ku Shizuoka, 422-8529, Japan
e-mail: acypark@ipc.shizuoka.ac.jp

M. Yui • T. Kato • E. Y. Park
Laboratory of Biotechnology, Department of Applied Biological Chemistry, Faculty of Agriculture, Shizuoka University
836 Ohya Shizuoka, 422-8529, Japan

M. Yamazaki • E. Y. Park
Graduate School of Science and Technology, Shizuoka University
836 Ohya Shizuoka, 422-8529, Japan

M. J. Alam • M. Yamazaki
Research Institute of Electronics, Shizuoka University
836 Ohya, Suruga-ku Shizuoka, 422-8529, Japan

to form VLPs and are incapable of infection because they are devoid of genetic material. Group antigen protein (gag) protein from *Rous sarcoma* virus (RSV) species belonging to the family *Retroviridae*, subfamily *Orthoretrovirinae*, genus *Alpharetrovirus* of single stranded RNA virus forms VLPs. gag protein used in the present study is composed of 577 amino acid length with 61 kDa molecular weight, devoid of the protease region (1). It is composed of a membrane-binding domain that directs the gag protein to the plasma membrane via a well-known lipid raft pathway conserved in retrovirus family (2,3). The interaction domain promotes gag-gag multimerization important for particle assembly to form the VLPs of approximately 80–100 nm and the late assembly domain later facilitates the pinching of viral particles enveloped in a lipid layer from the plasma membrane assisted by proteases (2,4). Lipid layer can be used to display membrane bound proteins on VLPs surface using glycosylphosphatidylinositol (GPI) anchor domain of proteins (5). The GPI moieties are widely spread in living organisms, playing significant role in providing varying biological functions (6). GPI-anchoring of the proteins takes place in the endoplasmic reticulum membrane at specific site recognized by enzymes enabling the protein to hitch a ride on lipid rafts and reach plasma membrane undergoing the post-translational changes (7,8). A simple but efficient process, the C-termini of protein covalently attached to GPI via fatty acid chain is stably associated with the membrane. Use of GPI anchored proteins is well-known for detection as well as for targeting disease-causing factors for therapy (9–11). GPI anchored antibodies on VLPs have not yet been studied but antibodies fused with GPI anchored in lipid membranes has been shown to be useful and effective against targets such as HIV-1 envelope spikes for neutralization (12).

Immunotherapy has been revolutionized by the successful screening and development of numbers of monoclonal antibodies (mAbs) against specific markers on cancer as a tool for therapy (13,14). CC49 is a clinically validated antibody to target a tumor-associated glycoprotein-72 (TAG-72) a well-known marker in colon carcinoma (15). mAbs coupled with or without toxins or chemical drugs have been marketed under different names like anatumomab, mafenatox and minretumomab as chemo-therapy treatment an alternative to surgical treatment method (16). mAbs conjugated to drugs or by themself when administered in patients to target tumors have less penetration and only 20% of the administered dose interacts with the tumors (14). mAbs also show clinical bottleneck of aggregation in kidney and other organs involved in removal of toxic materials due to extended biological half-life (2–3 weeks depending on class of antibody) in blood circulatory system (13,14). Alternatively, single-chain variable fragment (scFvs) linked by a short linker has shown high specificity and relatively low biological half-life (less than 2 h) allowing it to be used as a radio labeled molecule for imaging and diagnosing tumors in patients. Shorter retention time is also one of the main downfalls as the duration its available in the circulatory system is not enough for drug delivery. Different drug delivery systems using scFvs conjugated to drugs or fused with other proteins to be activated on site of target, increase its retention time and enhance the delivery of drug to tumor (15,17). The biggest disadvantage of such an approach is that modifying the protein by chemical process to tag the scFvs with drugs or enzyme fused with scFvs causes improper folding and loss of scFvs function (18). Hence here a novel approach of displaying recombinant scFvs (rscFvs) anchored with GPI embedded in the lipid layer of VLPs is studied.

The silkworm expression system uses silkworm larvae to express and purify proteins efficiently at milligrams level, using *Bombyx mori* nucleopolyhedrovirus (BmNPV), which belongs to the double-stranded DNA virus family *Baculoviridae* (1). BmNPV infects silkworms using spike proteins on baculovirus envelope, like glycoprotein 64 (GP64) a type I membrane protein to associate and fuse with cell membrane to infect silkworms (19–21). GP64 is further classified as type III membrane fusion protein class depending upon its fusion property of initiating fusion independently without any help by forming large fusion pores rapidly. Association of GP64 with membranes takes place first leading to fusion of GP64 to lipid membrane driven by protonation of Histidine amino acids (pK_a 6.0) (22,23). Previously, it has been reported that RSV gag VLPs expressed and purified using baculovirus expression system have GP64 peppered on its surface (24). Here the use of functional GP64 on VLPs and their association with large unilamellar vesicles (LUVs) membrane in developing a new drug delivery system is studied. The focus is on developing VLPs-rscFvs as a model drug delivery system associated with hydrophilic fluorescent dyes by LUVs. LUVs only packaged with either hydrophilic or hydrophobic fluorescent dyes are well known for studying drug delivery to 3D tumors spheroid model (25–27). The *ex vivo* 3D spheroid models offer a platform to study and gain insight into drug delivery properties of rapidly evolving new drug delivery tools. The major drawback of using LUVs alone packaged with drugs as a tool for therapy is the non-specificity and the toxicity resulting due to accumulation in detoxification related organs and tissue in humans. LUVs with various marker proteins or baculovirus fused with LUVs have been studied as a drug delivery tool (23,28). Such an approach has either high toxicity or due to use of large baculovirus which carries genetic material causes health and infection concerns and its use is curtailed. Hence the current study focus is on developing a new model system devoid of any genetic material with high target specificity provided by rscFvs anchored on VLPs by GPI carrying a test fluorescent dye.

In the current study, feasibility of using VLPs a macromolecular structure displaying rscFvs targeting cancer cells and spheroids made from the same cells has been tested. The current approach uses GPI to anchor scFv on VLPs without

putting any protein folding constraints on either scFv-GPI or gag-gag multimerization for VLPs formation. In addition, LUVs packaged with sulforhodamine B (SRB) a water-soluble fluorescent dyes to associate with VLPs displaying rscFv and GP64 as a model to test an effective drug delivery. SRB a water soluble negatively charged aminoxanthine dye is used for cell based cytotoxicity assay in various cancer cell lines with better accuracy than other known assay (29). Utilizing GP64 is important for large-scale application because VLPs displaying rscFvs can be made with ease by the silkworm expression system and the VLPs can serve as carrier of drugs or dyes to give the extra merit needed in rapidly evolving drug delivery systems targeting tumors.

MATERIALS AND METHODS

Cell Lines and Media

LS174T human colon adenocarcinoma cell line (ATCC CL-188) was obtained from ATCC (Manassas, VA, USA) and HEK293 (RCB1637) was obtained from Riken Bio Resource Center (Tsukuba-shi, Ibaraki, Japan). LS174T presenting a tumor associated glycoprotein-72 (TAG-72) on cell surface, was cultured in 60 mm culture plates (TPP, Trasadingen, Switzerland) with MEM-eagle medium (Sigma-Aldrich, St. Louis, MO, USA) containing 10% (v/v) fetal bovine serum (Invitrogen, Carlsbad, CA, USA), supplemented with 1% (v/v) antibiotic solution containing penicillin, streptomycin, fungizone (Sigma-Aldrich) and incubated at 37°C in 5% CO_2 incubator (MCO-175 Sanyo, Osaka, Japan). HEK293 were cultured in 60 mm culture plates with MEM/EBSS (HyClone Laboratories Inc., Utah, USA) containing 2 mM L-glutamine, 1% non-essential amino acid (Invitrogen), 10% fetal bovine serum, supplemented with 1% (v/v) antibiotic solution containing penicillin, streptomycin, fungizone and incubated at 37°C in 5% CO_2 incubator. Both the cell lines were grown till confluence and splitting was done in 1 : 5 ratio once every week by trypsinisation using TrypLE Express (Life Technologies Japan LTD., Minato-Ku, Tokyo, Japan) for 15 min at 37°C in 5% CO_2 incubator.

PCR Amplification and Bacmid Preparation

Using PredGPI software the GPI anchor position and the nucleotide sequence was confirmed as previously reported for VLPs displaying rNcSRS2 (7) and the same GPI anchor is used in current work. The plasmid carrying CC49 gene was kindly provided by Professor Hiroshi Ueda (Tokyo Institute of Technology, Japan). The scFv cDNA was cloned by PCR into pENTR to make pENTR/scFv-DDDDK. The GPI anchor cDNA was inserted in frame by PCR using pENTR/scFv-DDDDK plasmid as template using forward primer 5′-caccatg**aagatactccttgctattgcattaatgttgtcaacagtaatgtg-ggtgtcaacagactacaag**gatgacgatgacaag-3′ and reverse primer 5′-ttatcagtacgcaaagattgccgttgcagtcagtgac gcagcggatagtgccacgtacgaaggcaactcgtcacatgcatctccggat ccccccccccgtttaa-3′ respectively. The forward primer contained 63 base pair Bombyxin signal (bold) sequence followed by DDDDK affinity tag nucleotide sequence (dashed line). The reverse primer contained the 81 base pair of putative GPI signal (underlined) motif of NcSRS2. PCR products were inserted into the entry vector, pENTR/D-TOPO (Invitrogen) to give pENTR/scFv-GPI. The PCR fragment inserted into pENTR/D-TOPO was confirmed by dideoxynucleotide chain terminating sequence (30) using Thermo Sequenase Cycle Sequencing kit (USB Co., Cleveland, Ohio, USA). pENTR/scFv-GPI was used to transfer scFv-GPI to pDEST8 by LR reaction according to the protocol to make pDEST8/scFv-GPI, which was used to transform to *E. coli* BmDH10bac competent cells to make recombinant bacmids (31). White colonies of recombinant bacmid carrying scFv-GPI gene were isolated and resulting bacmid was designated as BmNPV bacmid/VLP-rscFvs**.**

Bacmid/RSV-gag-577 from previously reported work is used (1) and the BmNPV bacmids were isolated and resuspended in phosphate buffered saline containing 80 mM disodium hydrogen orthophosphate anhydrous, 19 mM sodium di-hydrogen orthophosphate anhydrous, and 100 mM sodium chloride (PBS, pH 7.5) for injection.

Silkworm Larvae Rearing, Feeding and Injection

Fifth instars larvae (Ehime Sansyu Co. Ltd., Ehime, Japan) were reared on an artificial diet Silkmate S2 (Nihon Nosan Kogyo, Yokohama, Japan) in a 65% humidity chamber (MLR-351H, Sanyo, Tokyo, Japan) at 27°C.

Each silkworm was injected with 40 µL recombinant bacmid DNA solutions containing 10 µg of BmNPV-gag577 and BmNPV-scFv-GPI bacmids, respectively, in 10% (v/v) DMREI-C reagent (Invitrogen) in PBS using 1 mL syringe. Post injection 7th day the silkworm larval hemolymph was harvested in tubes (Falcon, Lincoln Park, NJ, USA) containing 2 mM phenyl thiourea and complete EDTA-free protease inhibitor cocktail to inhibit the hemolymph melanization and protein degradation by proteases. These samples were aliquoted into eppendorf tubes and stored at −80°C.

Purification of VLPs Displaying scFvs-GPI

VLP-rscFvs containing hemolymph collected from silkworm larvae were centrifuged at 1,000 g in a Heraeus Primo R Sorvall Biofuge (Thermo Scientific, Yokohama, Japan) for 3 min using Heraeus 7591 swing bucket rotor to remove debris. The clear hemolymph was dialyzed with cellulose ester

dialysis membrane (Spectrum Laboratories Inc., California, USA) having 300,000 molecular weight cut off in 2 L of PBS (pH 7.5) for overnight at 4°C. The dialyzed hemolymph was centrifuged at 14,010 g using micro refrigerated centrifuge (Model 3700, Kubota, Tokyo, Japan) for 10 min at 4°C to remove any aggregates and the supernatant was filter-sterilized with 5 μm filter membrane (Merck-Millipore, MA, USA). The protein sample was added to PBS pre-equilibrated 5 mL of DDDDK-agarose gel (Medical and Biological Laboratories Co., Ltd., Nagoya, Japan) in batch mode and purification performed as per the kit protocol. Elution was carried out using 0.1 mg/mL DDDDK peptide (Medical & Biological Laboratories Co., Ltd., Nagoya, Japan) in 500 μL aliquots. The protein concentrations were measured using standard BCA protein estimation kit (Pierce BCA Assay kit, IL, USA).

Western-Blot Analysis

To detect the expression of VLPs and rscFvs, larval hemolymph from silkworm larvae were collected. Samples were subjected to 10% (w/v) SDS-PAGE using the mini-protean II system (Bio-Rad, Hercules, California, USA). After SDS-PAGE, proteins were blotted on to a PVDF membrane using the Mini Trans-Blot Electrophoretic Transfer cell (Bio-Rad) at 15 V for 1 h. The membranes were probed with 5,000 and 2,000 fold diluted mouse anti-DDDDK primary antibodies (Wako Pure Chem. Ind. Ltd., Osaka, Japan) for rscFvs and rabbit anti-RSV-gag primary antibody for gag-577 (1), respectively, in Tris-buffered saline with 0.1% (v/v) Tween-20 (TBS-T) (Wako) for 1 h at room temperature with mild shaking. Secondary antibodies conjugated with horseradish peroxidase (HRP) were goat anti-mouse IgG (Santa Cruz Biotechnology, Santa Cruz, CA, USA) for rscFvs and goat anti-rabbit IgG (Santa Cruz Biotechnology) for gag-577, respectively. The secondary antibodies were incubated for 1 h at room temperature and specific bands for rscFvs and gag-577 proteins were detected using an Immobilon western blotting reagent pack (Millipore Corporation, Billerica, Massachusetts, USA). The rscFvs and gag-577 proteins bands were analyzed using a Fluor-S/MAX multi-imager (Bio-Rad).

Confirmation of the Antigen Specificity of rscFvs Displayed on VLPs by ELISA

Human TAG-72 at 20 U per well (Sigma-Aldrich) in 100 μL volume was immobilized in an immuno plate (Thermo Scientific, West Palm Beach, FL, USA), overnight at 4°C in triplicates. The plates were blocked with 100 μL/well Ez-block Chemi (ATTO Co., Tokyo, Japan) for 1 h at room temperature and washed thrice with 200 μL/well PBS (pH 7.5). Five micrograms of VLP-rscFvs and VLPs were added to each well, respectively and incubated for 2 h at room temperature. After incubation, the plates were washed three times with 200 μL/well PBS (pH 7.5). The plates were incubated with 100 μL/well mouse anti-DDDDK antibody 2,000 fold diluted in PBS-T (Tween-20 0.1% (v/v)) and incubated for 1 h at room temperature. After incubation the plates were washed thrice with 200 μL/well PBS-T pH 7.5 and incubated with goat anti-mouse IgG conjugated with HRP 4,000 fold diluted in PBS-T for 1 h at room temperature. After incubation the plates were washed thrice with 200 μL/well PBS-T (pH 7.5) and detection was carried out using 3,3′-,5,5′-tetramethylbenzidine (TMBZ) (Dojindo, Kumamoto, Japan) solutions by observing the absorbance at 450 nm by Plate reader (Bio-Rad) (5).

Phospholipase C Treatment of VLP-scFv-GPI

Each well of immuno plate was immobilized with 5 μg of VLP-rscFvs and VLPs, respectively for overnight at 4°C in triplicates. The plates were blocked and treated with primary and secondary antibodies similar to ELISA method. After incubation the plates were washed three times with 200 μL/well PBS-T (pH 7.5) and presence of the GPI anchor from the lipid layer was confirmed by digestion with 0.1 U of phosphatidyl-inositol specific Phospholipase C (PI-PLC) (Sigma-Aldrich) in 200 μL/well PBS (pH 7.5) for 2 h at 27°C. After incubation the plates were washed and scFv was detected similar to ELISA method.

Hemolysis Assay

Rabbit erythrocytes (Nihon BioTest Research, Tokyo, Japan) were prepared and 2.5% (v/v) were seeded per 96-well plate in triplicates (32). Purified VLP-rscFvs and Bovine serum albumin (100 μg/mL) as a negative control were added and allowed to absorb for 10 min on ice. Then, the mixture was incubated for 30 min at 37°C. Extent of hemolysis was determined spectrophotometrically at 540 nm in a plate reader (Bio-Rad).

Liposome Preparation and Sulforhodamine B Packaging

Multilamellar vesicles (MLVs) were prepared using 10 mM 1,2-dioleoyl-*sn*-glycero-3-phosphocholine (DOPC) (Avanti Polar Lipids, Alabaster, Alabama, USA) dissolved in chloroform (Wako) in 5 mL glass vial with a cap. DOPC was evaporated under flowing nitrogen gas, films formed at the bottom of the vial and were kept in a desiccator in vacuum overnight for complete drying of chloroform. Films were then hydrated by adding PBS (pH 7.5) containing 1 mM sulforhodamine 101 acid chloride (SRB) (Dojindo, Kumamoto, Japan) at room temperature by vortexing five times for 20 s. SRB was packaged into MLVs by freeze thawing method in a three-step cycle of 20 min. MLVs were extruded using Avanti Mini-extruder (Avanti Polar Lipids)

with a 19 mm diameter polycarbonate 100 nm pore size membrane (Avestin, Ontario, Canada) 20 times to produce LUVs packaged with SRB (LUV-SRB). LUV-SRB mixture containing LUVs and LUVs-SRB were resolved on pre-equilibrated sephadex G75 (7 cm × 3 cm dimensions) column (Terumo, Tokyo, Japan). The purified LUV-SRB suspension was collected from the void volume fraction and concentration of the lipid and SRB were estimated (33). Lipid estimation was done by Fiske-Subbarrow colorimetric method using LUV-SRB prepared in HEPES buffer pH 7.5 under conditions similar as described above. The SRB excitation and emission measurements were taken at 515 and 604 nm, respectively by a 96 well spectrophotometer (Tecan Japan Co., Ltd., Kawasaki, Japan).

One hundred micrograms of VLP-rscFvs in 500 μL of PBS (pH7.5) buffer were mixed with 500 μL of LUV-SRB containing 28.8 μM DOPC and 1 mM SRB. The mixture VLP-rscFv-LUV-SRB (VLP-rscFv-SRB) was incubated for 1 h at 27°C for association to be complete. Small aliquot from VLP-rscFv-SRB sample was used for SRB concentration measurement.

Dynamic Light Scanning (DLS) Measurement

One hundred micrograms of purified VLP-rscFvs and VLP-rscFv-SRB were extruded using Avanti Mini-extruder (Avanti Polar Lipids) with a 19 mm diameter polycarbonate 200 nm pore size membrane (Whatman Japan Ltd., Tokyo, Japan) three times to get uniformly dispersed sample. The samples were loaded in disposable cuvettes (DTS-1061) for measurement of size with the Zetasizer Nano series (Malvern, Worcestershire, United Kingdom).

Transmission Electron Microscopy (TEM) of VLP-scFvs-GPI and its Packaging

The purified VLPs-rscFvs, LUV-SRB and VLP-rscFv-SRB samples respectively were spotted on carbon grids (Okenshoji, Tokyo, Japan) and dried at room temperature. Negative staining was performed using 2% (v/v) phosphotungstic acid (Wako) as described previously (5). For immunoelectron microscopy, VLPs-rscFvs and VLP-rscFv-SRB samples were loaded on the grids in similar fashion and the grids were blocked using 4% (w/v) bovine serum albumin (BSA) (Sigma-Aldrich) for 1 h and washed with PBS (pH 7.5). The grids were incubated in PBS containing mouse anti-DDDDK at 1:100 dilutions for 2 h, and washed with PBS. Subsequently, the grids were incubated in PBS containing 1:200 diluted goat anti-mouse IgG conjugated with 10 nm gold particles (BB International, Cardiff, UK) for 2 h, and washed with PBS. Negative staining was performed as mentioned above and samples were observed at 50,000 × magnification (JEM 2100F-TEM, JEOL Ltd., Akishima, Tokyo, Japan) operating at 200 kV. The high-resolution TEM images were transformed using fast Fourier transformation function available with the instrument.

Confirming Specificity of VLP-rscFvs

LS174T and HEK293 cell lines were cultured for 3 days and around 10^4 cells were seeded on glass slides (2.6 cm × 7.6 cm) (Matsunami Glass Ind., LTD., Osaka, Japan) and incubated overnight under growing conditions. The cells were washed respectively with fresh medium and incubated with 3 μg of VLP-rscFvs for 3 h. The cells respectively were treated with 500 fold diluted BODIPY FL-C5-ceramide conjugated to BSA (Invitrogen) and mouse monoclonal anti-DDDDK-tag-Alexa Fluor 594 (MBL Co. LTD., Nagoya, Aichi, Japan) respectively and incubated for 1 h at 37°C. The cells were then washed with fresh growth medium and incubated with 1,000 fold diluted 4′-6-Diamidino-2-2-Phenylindole, Hydrochloride (DAPI) solution for 1 h at 37°C. The cells were washed once respectively, fixed using 2% (v/v) formaldehyde and viewed under confocal laser scanning microscope (CLSM) (LSM 700, Carl Zeiss, Oberkochen, Germany) with Plan-apochromat 40 × (2.5 zoom factor) oil lens respectively. Zen LE software available on Carl Zeiss website was used for image analysis.

Similar amount of VLP-rscFvs as used above was also fixed on glass slides and treated with 500 fold diluted mouse monoclonal anti-DDDDK-tag-Alexa Fluor 594 and incubated for 1 h at 37°C. VLP-rscFvs samples were not stained with DAPI as there was no nucleus present. The samples were fixed as mentioned above and observed under CLSM with Plan-apochromat 100 × (1 zoom factor) oil lens. Zen LE software available on Carl Zeiss website was used for image analysis.

Delivery of VLP-rscFv-SRB

LS174T cells as mentioned above were cultured and seeded on the slides. The cells were washed with fresh medium and incubated with 3 μg of VLP-rscFv-SRB and 100 μL of LUV-SRB as a negative control for 3 h. The cells were washed and treated with 500 fold diluted mouse monoclonal anti-DDDDK and incubated for 1 h at 37°C. The cells were washed and treated with 1000 fold diluted FITC conjugated goat anti-mouse IgG (Jackson ImmunoResearch lab., Baltimore, Maryland, USA) and incubated for 1 h at 37°C. The cells were washed once respectively, fixed using 2% (v/v) formaldehyde and viewed under CLSM with Plan-apochromat 100 × oil lens and 20 ×, respectively. Zen LE software available on Carl Zeiss website was used for image analysis.

Large Spheroids Preparation and VLP-rscFv-SRB Delivery

Large spheroids mold of 0.8 mm×0.8 mm (diameter × depth) with 5×7 array using 3D Petri dish (MicroTissues Inc., Rhodes Island, USA) were used to produce 500 μm diameter spheroids as per kit protocol. LS174T cells resuspended in 200 μL growth medium (1.4×10^5 cells) were applied to equilibrated spheroid molds kept in 60 mm cell view cell culture plates (Greiner Bio-one GmbH, Maybachstr. 2, Germany) and incubated at 37°C in CO_2 incubator for 30 min resulting in large spheroid formation, confirmed with 2×lens of Olympus SZX14 microscope (Olympus, Tokyo, Japan).

One hundred micrograms of VLP-rscFv-SRB mixture were added to spheroids and incubated at 37°C in CO_2 incubator for 3 h. The spheroids were then washed with growth medium and treated with 250 fold diluted mouse monoclonal anti-DDDDK in 500 μL growth media and incubated at 37°C in CO_2 incubator for 1 h. The spheroids were washed with fresh growth medium and treated with 500 fold diluted goat anti-mouse IgG (H+L) conjugated with FITC (Jackson ImmunoResearch lab.) in 500 μL growth medium and incubated at 37°C in CO_2 incubator for 1 h. Finally the cells were washed with growth medium and observed under live condition using 10 × apochromat lens of CLSM. Z-stacking was performed for 338 μm in-depth of spheroid with each cross-sectional scanned layer of 1 μm. All the Z-stacked images collected were rendered to prepare the 3D model using Zen LE 2011 version software available on Carl Zeiss website.

RESULTS

Expression and Purification of rscFvs and Gag Proteins

Expression of rscFvs (~32 kDa) and gag protein was confirmed in purified samples collected from silkworm larvae hemolymph co-injected with both BmNPV/RSV-gag-577 and BmNPV/rscFvs bacmids. The western blot data for gag confirmed with molecular weight as reported earlier (Fig. 1a) (4). The western blot data for rscFvs shows another 35 kDa band (Fig. 1b), the apparent increase by about 3 kDa results due to the cells inability to remove the Bombyxin signal sequence or the GPI anchor whose processing might be one of the reasons. Approximately 1.5 mg of purified VLP-rscFvs was isolated from 30 mL of silkworm larvae, and shows the presence of the rscFvs and gag bands in CBB stained SDS-PAGE gel (Fig. 1c).

Confirmation of Antigenicity and GPI Anchorage

The rscFvs specificity to bind to TAG-72 the marker on colon carcinoma is an important property. The antigen specificity of rscFvs was confirmed by ELISA using TAG-72 antigen. Compared to negative control without rscFvs, specificity of VLP-rscFvs for TAG-72 was 22 fold higher (Fig. 2a).

The GPI anchorage of rscFvs was investigated using PI-PLC treatment. PI-PLC treated wells compared to untreated wells showed around 40% decrease in signal (Fig. 2b) indicating presence of GPI anchored scFv. VLPs only as negative control show no remarkable change.

TEM and ImmunoTEM Analysis of VLP-scFvs and VLP-rscFv-SRB

TEM images of purified VLPs-rscFvs show a distinctive bilayer that is usually present on enveloped VLPs with a diameter of 100 nm (Fig. 3a). The immuno-TEM images of VLP-rscFvs show presence of rscFvs particles on the surface of VLPs (Fig. 3b). TEM images of purified LUVs packaged with SRB shows distinctive smooth shaped LUVs of approximately100 nm in diameter (Fig. 3c). TEM images of VLP-rscFv-SRB associated with LUVs-SRB shows the lipid bilayer. The average size of VLP-rscFv-SRB from TEM images is around 120–150 nm in diameter (Fig. 3d). Immuno-TEM of VLP-rscFv-SRB shows presence of rscFvs particles on the surface of VLP-rscFv-SRB (Fig. 3e). VLP-rscFv-SRB TEM images show the association between VLP-rScFvs and LUV-SRB as shown by the arrows (Fig. 3f). Both VLP-rscFv-SRB and LUV-SRB have a high contrast but the distinctive bilayer of VLPs easily distinguishes the nanostructures and suggests that VLP-rscFvs can bind strongly to LUV-SRB at pH 7.5. The samples were passed through 200 nm nucleopore membrane to avoid aggregation among VLP-rscFvs before measuring size by DLS for quantitative analysis of size change. The peak of the number distribution for the diameter of LUV-SRB, VLP-rscFvs and VLP-rscFv-SRB from DLS data was around 68, 51, and 79 nm, respectively (Fig. 3g). The shift in diameter for VLP-rScFvs and VLP-rscFv-SRB from DLS was of 28 nm. The increase in diameter of VLP-rscFv-SRB might be due to association or fusion of LUV-SRB with VLP-rscFvs suggesting that VLP-rscFvs can bind strongly to LUV-SRB at pH 7.5. LUV-SRB association with VLP-rscFvs results due to presence of GP64 on VLP-rscFvs surface.

The result of hemolysis indicates that VLP-rscFvs-SRB associated with RBCs strongly to induce hemolysis at pH 7.5 (Fig. 4), suggesting that VLP-rscFvs can bind strongly LUV-SRB. The negative control using BSA showed zero percent hemolysis (Data not shown).

Localization of VLP-rScFvs and VLP-rscFv-SRB

Purified VLP-rscFvs were viewed under CLSM, and 0.1–0.2 μm big spots were observed after treatment with Alexa Fluor 594 conjugated anti-DDDDK (Fig. 5a–c), supporting that the presence of rscFvs in purified VLP-rscFvs as shown in

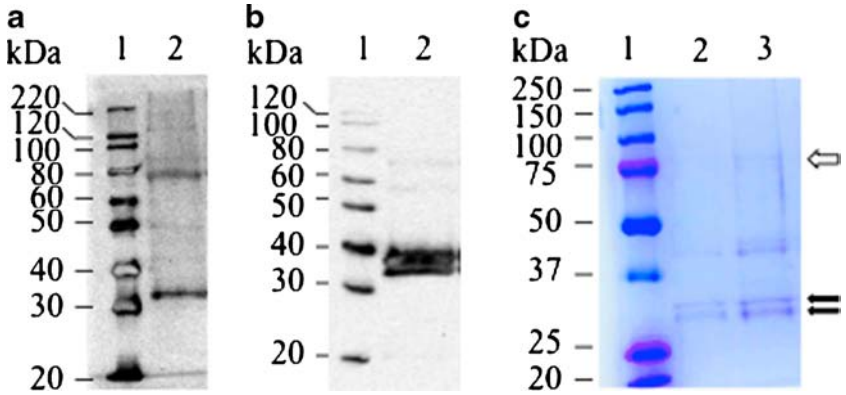

Fig. 1 Western blotting of purified samples of VLP-rscFvs. gag-577 (**a**) and rscFvs (**b**) were detected by western blotting using rabbit anti-gag primary antibody and mouse anti-DDDDK primary antibody, respectively. Secondary antibodies used for detection of gag-577 (**a**) and rScFvs (**b**) were goat anti-rabbit IgG and goat anti-mouse IgG, respectively. Lane 1: molecular weight marker; lane 2: 1 μg of VLP-rscFvs samples. **c** CBB stained 10% SDS-PAGE gel of VLP-rscFvs samples. Lane 1: molecular weight marker, lanes 2 and 3: 1 μg and 5 μg of VLP-rscFvs samples, respectively. The *black* and *white arrows* show the rscFvs and gag (some minor cleaved bands of gag are also observed between 40 and 61 kDa), respectively.

the schematic representation (Fig. 5d). The purified VLP-rscFvs show specificity to the TAG-72 antigen present on LS174T cells surface (Fig. 6a–d). The rscFvs presence and its localization were confirmed in LS174T cells (Fig. 6c and d). As a negative control, LS174T cells were treated with VLPs without rscFvs and they show no fluorescence for the affinity tag of scFv (Fig. 6e–h). Purified VLP-rscFVs was added to HEK293 cells to further confirm the specific binding of the VLP-rscFvs irrespective of any influence from lipid layer around VLPs, shows only plasma membrane localizing dye and no fluorescence for rscFvs (Fig. 6i–l). Thus VLP-rscFv can bind to LS174T cells specifically via scFv for TAG-72 antigen.

Association of VLP-rscFvs with SRB and Targeting the Cells and Spheroids

LS174T cells with and without VLP-rscFvs-SRB treatment confirmed the delivery of SRB to cells (Fig. 7a–f). Approximately 3 µg of VLP-rscFvs-SRB treated cells show FITC fluorescence for the affinity tag of rscFvs and SRB, respectively (Fig. 7a and b). In negative control cells treated with LUV-SRB or 1 mM SRB only showed insignificant fluorescence of FITC and SRB (Fig. 7d–e and Supplementary Fig. 3). VLP-rscFvs-SRB binding to cancer cells is facilitated by rscFvs specificity for TAG-72, leading to the delivery of SRB the test model dye to cell (Supplementary Fig. 1).

Large spheroids of 500 µm in diameter were produced using 3D agarose scaffold (5×7 arrays) (Supplementary Fig. 2). The spheroids were spherical and there was no aggregation of cells on the scaffold body other than the intended area. Approximately 2.8 µg of VLP-rscFv-SRB per spheroid was incubated and fluorescence of SRB and FITC channels was observed as shown schematically from bottom (Fig. 8a). All the images for Z-stacking of 1 µm thickness were taken from the bottom to top. The rendered images showed SRB at a depth of 100–150 µm from the bottom of spheroid (Fig. 8b). FITC denoting rScFvs was observed at a depth of about 150–250 µm from the bottom of the spheroid (Fig. 8c). The depth indicator from the merged picture shows there is overlap

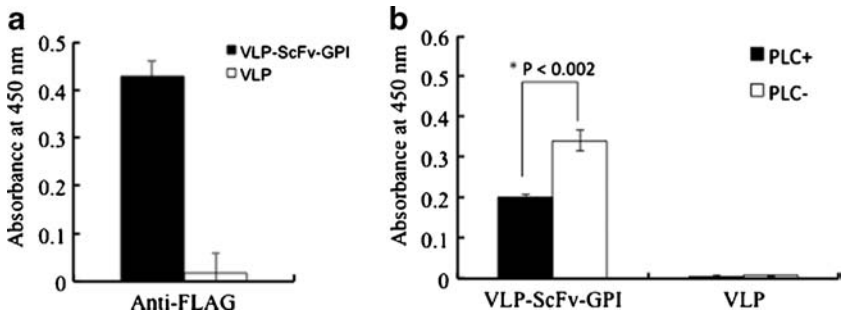

Fig. 2 (**a**) Confirmation of antigenicity was tested using 20 U of TAG-72 per well. Five micrograms per well of purified VLP-rscFvs protein samples were loaded and the wells were probed with mouse anti-DDDDK and secondary antibodies were goat anti-mouse IgG for rscFvs. *Black* and *white bars* denote VLP-rscFvs and VLPs samples, respectively. Data are the mean ± SD ($n = 3$) (**b**) Presence of GPI anchor was confirmed by PI-PLC treatment by ELISA method. *Black* and *white bars* represent with and without PI-PLC wells. Data are the mean ± SD ($n = 3$).

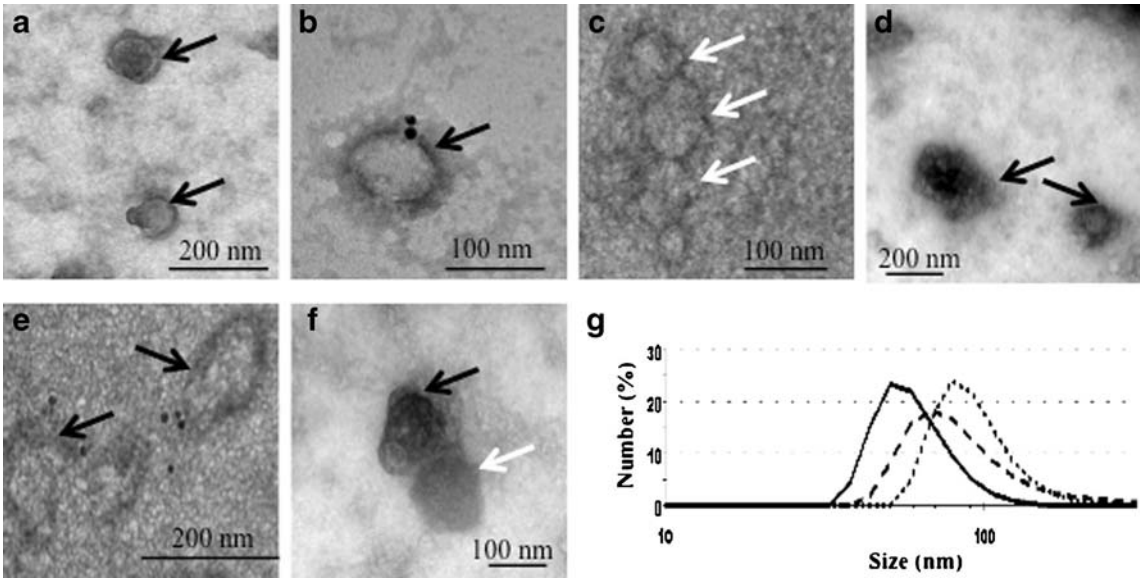

Fig. 3 TEM and immuno-TEM pictures. (**a**) VLP-rscFvs. Scale bar is 200 nm. (**b**) VLP-rscFvs with 10 nm gold particles. Scale bar is 100 nm. (**c**) LUV-SRB. Scale bar is 100 nm. (**d**) VLP-rscFv-SRB. Scale bar is 200 nm. (**e**) VLP-rscFv-SRB with 10 nm gold particles. Scale bar is 200 nm. (**f**) VLP-rscFv-SRB showing association. Scale bar is 100 nm. *Black arrows* denote distinctive bilayer of VLPs. *White arrows* indicate LUVs-SRB. (**g**) DLS data of LUV-SRB (*long dash line*), VLP-rscFvs (*solid line*) and VLP-rscFv-SRB (*short dash line*). One hundred micrograms of VLP-rscFvs and VLP-rscFv-SRB were used for assay, showing the shift in size (diameters in nm) before and after association.

between SRB and rScFvs respectively at 100–150 μm from the bottom as observed by the yellow color due to mixing of red and green channel colors (Fig. 8d). SRB (Fig. 8b) fluorescence and scFvs signals (Fig. 8c) were overlapped on the surface of the spheroid, indicating that scFv-displaying VLP bound to the cells on the surface of LS174T spheroid and carried SRB to these cells.

DISCUSSION

Many kinds of drug delivery systems targeting tumors for therapy using liposome's and VLPs of different compositions and proteins are being developed for delivering genes or drugs to mammalian cells (16,34,35). Here the novel use of VLPs displaying rScFvs with SRB as a model dye was reported to confirm the hypothesis of using VLP-rscFvs as a new drug delivery system. In order to develop the delivery system an expression system using silkworm larvae was established and VLP-rscFvs expression and purification in milligram levels was confirmed. rscFvs expression and its display on the VLPs was facilitated by bombyxin signal sequence from *Bombyx mori* added to N-Terminal side of rscFvs (5). The signal sequence facilitates the rscFvs to reach the plasma membrane where VLPs formation takes place and they are secreted into silkworm larval hemolymph. gag protein shows different bands due to protease activity present in silkworms hemolymph as shown before (4,17,22). gag (~42 kDa) protein can be confirmed by CBB staining but the other band intensities were low for detection by CBB staining.

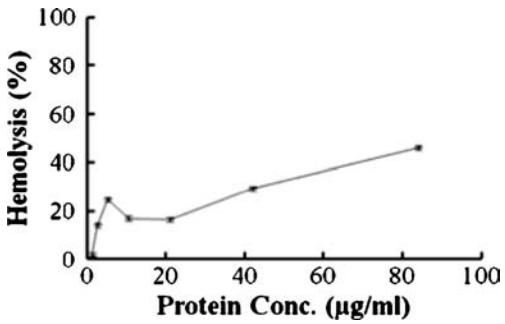

Fig. 4 Purified VLP-rscFv was used to qualitatively evaluate GP64 functions by hemolysis assay. Rabbit erythrocytes when come in contact with GP64 a pore forming protein causes an increase in porosity of the membrane leading to leakage of heme into supernatant, which is measured colorimetrically.

Many reported approaches use scFvs conjugated to drugs or proteins, but bottleneck of efficient conjugation and the resulting loss of function is a leading cause for less use of scFvs for therapy (14). In the present study, the high specificity of rscFvs displayed on VLPs is directly related with proper folding as there is no loss of function. The current protein expression model expresses two or more proteins independent of each other and the assembly takes place on the plasma membrane independent of each other with no protein folding constraints due to fusion. Thus the assembled proteins retain their native structures and functions. gag protein self assembly is well documented, its well suited for forming VLPs and display of foreign proteins (1,5). Use of GPI anchor to display protein embedded in VLPs lipid bilayer and retaining the high antigenicity at the same time has been reported previously (5).

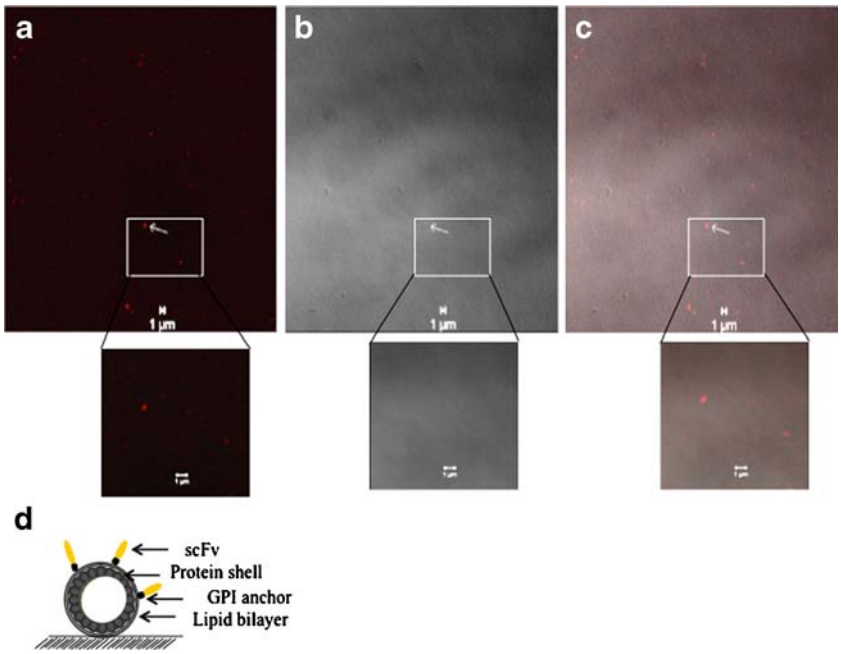

Fig. 5 VLPs-rscFvs were observed by CLSM after treatment with Alexa594 conjugated anti-DDDDK (**a**), in bright field image (**b**) and the merged image (**c**). Scale bar is 1 μm. (**d**) Schematic representation of VLP-rscFvs on the glass slide.

In the present study, a novel strategy employing GPI anchored scFvs on macromolecular nano-structures is tried. GPI anchoring was confirmed by PI-PLC treatment, an enzyme specifically cleaving the phosphodiester bond anchoring the protein to fatty acid chains in lipid layer of VLPs. The high antigen specificity of rscFvs against TAG-72 showed that the displayed protein is properly folded with no loss in function due to anchoring. VLP-rscFvs and VLP-rscFv-SRB displaying rscFvs was confirmed by TEM and the qualitative analysis of TEM images shows the size increase. To understand the size increase of VLP-rscFv and VLP-rscFv-SRB a quantitative analysis using DLS was done, which showed a spread out in

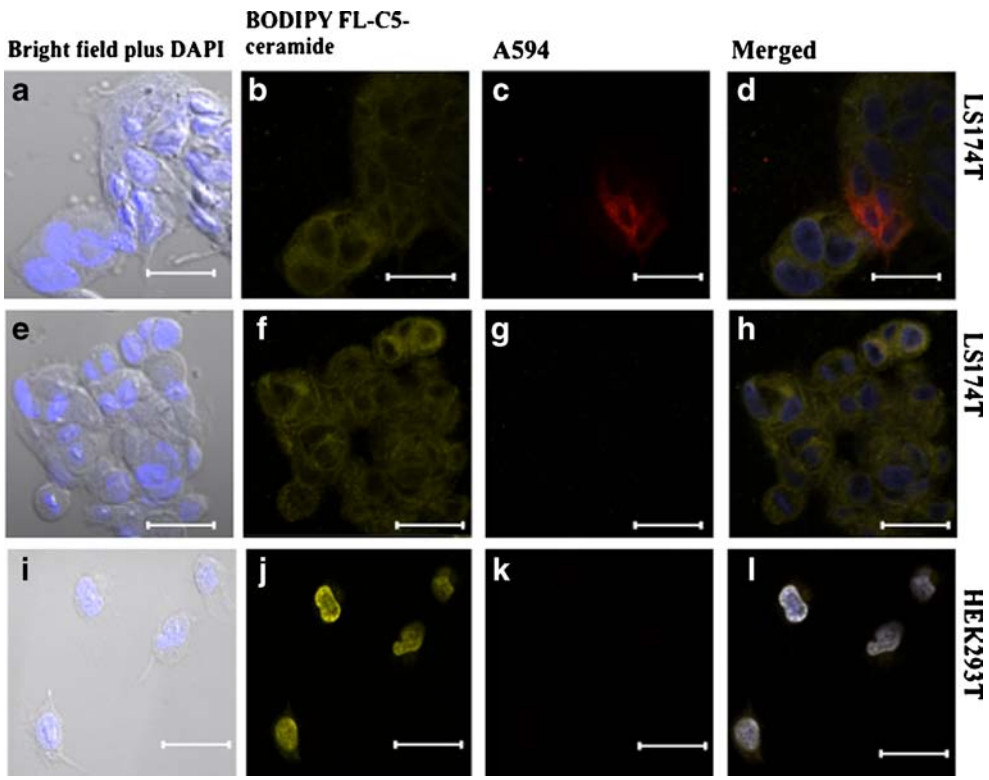

Fig. 6 CLSM pictures of LS174T cells with VLP-rscFvs (**a**–**d**), with VLPs (**e**–**h**), and HEK293T cells with VLP-rscFvs (**i**-**l**), respectively. (**a**, **e**, and **i**) DAPI and bright field overlapped image. (**b**, **f**, and **j**) BODIPY FL-C5-ceramide complexed to BSA for plasma membrane localization. (**c**, **g**, and **k**) Alexa594 conjugated anti-DDDDK for rscFvs. (**d**, **h**, and **l**) Merged images of all the color channels. Scale bars denote 20 μm.

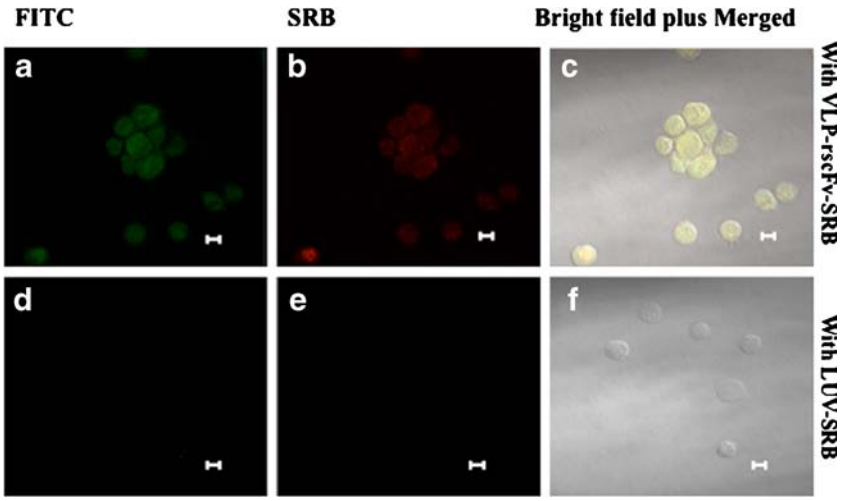

Fig. 7 CLSM pictures of LS174T cells with (**a**–**c**) and without (**d**–**f**) VLP-rscFv-SRB treated for co-localization studies. (**a** and **d**) FITC-conjugated goat anti-mouse IgG against mouse anti-DDDDK image. (**b** and **e**) SRB image and (**c** and **f**) bright field plus merged images of all the color channels. Scale bars denote 5 μm.

size as the current, expression system produces VLPs of varying size displaying different number of proteins. The exact mechanism involved in the current method to produce VLP-rscFv-SRB is unclear leading to association of LUV-SRB with VLP-rscFv and further work is needed.

Small scFvs anchored using GPI on VLPs can serve as an important tool for targeting cancer markers and support a robust delivery system. Here we propose using VLP-rscFv-SRB a composite macromolecular nanostructure with SRB to be delivered to spheroids *in vitro* as a model. The shape of the VLPs-rscFvs was similar as that of the VLPs (24). During the assembly of the macromolecular nanostructure GP64 is also peppered on top of VLPs due to the use of BmNPV expression system in silkworms as reported before (24). The apparent increase in diameter of VLPs-rscFvs could be attributed to insertion of the rscFvs and GP64 protein molecules together in between the gag monomers when the macromolecular nanostructure assembly takes place. The mechanism and number of proteins inserted per VLPs is not clear and needs to be further investigated. But GP64 is a well-studied fusion protein that forms large pore and due to presence of GP64, VLP-rscFvs with relative ease could be associated with SRB using LUV-SRB at neutral pH. To support this hypothesis GP64 function peppered on VLP-rscFvs was confirmed by hemolysis assay. The exact mechanism behind the association using LUV-SRB and VLP-rscFv needs to be further studied. rscFvs presence was confirmed on VLPs before and after fusion with LUVs-SRB. Association of dye did not influence presence of rscFvs opening the prospect of displaying multiple proteins on top of VLPs to target various types of tumors in future.

Cancer cell based assay reported here uses the binding specificity of VLP-rscFvs to TAG-72 present on the cancer cells surface. As a negative control HEK293 cells were used without any TAG-72 on its surface to show the binding specificity. The binding specificity to TAG-72 on cancer cell

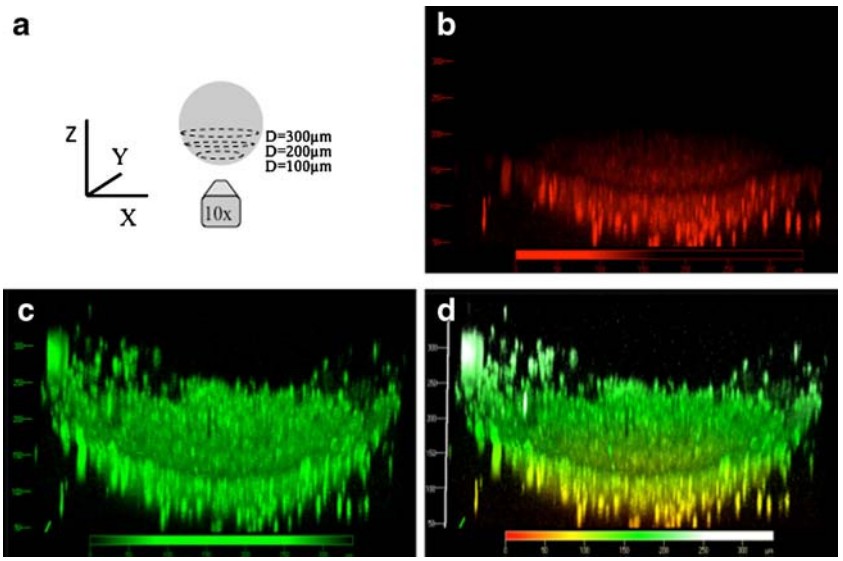

Fig. 8 The rendered color-coded depth projection of the entire z-stack of x-y images ($n = 338$) for the spheroid. (**a**) The schematic representation to show the lens position and the Z-stacking position. (**b**) Color coded depth projection of SRB. (**c**) Color coded depth projection of rscFvs. (**d**) Merged image of (**b**) and (**c**).

plasma membrane was confirmed by co-localization studies using membrane-localizing dye. VLP-rscFv-SRB functional property of binding was also confirmed in a similar manner with cancer cells, which confirmed association of LUV-SRB to VLP-rscFv, does not hinder in the binding specificity of rscFv. Here we propose a hypothesis wherein the rscFvs on VLP-rscFv-SRB bind with TAG-72 present on the cells leading to the delivery of the dye to cells (Supplementary Fig. 1). The presence of both SRB and rscFv co-localization takes place as observed by the merged yellow color resulting due to mixing of red and green color channels of the dye. Based on this hypothesis VLP-rscFv-SRB delivery of SRB to spheroids were confirmed by the co-localization of rscFvs and SRB. The presence of both SRB and rscFvs and its depth in the spheroids based on the rendered image generated using the z-stacked image is about 100–150 μm within 3 h of the incubation period. SRB is well known for cancer cell cytotoxicity assay studies owing to its sensitivities but the primary motive here was to show the delivery of the dye to the spheroids. The endocytosis pathway and the penetration property of the fluorescent probe SRB needs to be further investigated. In the current research it was used as a model for confirming the delivery only.

CONCLUSIONS

This study shows two novel aspects, first is the novel use of GPI anchors successfully displaying rscFvs on top of VLPs. By placing rscFvs specific towards TAG-72 displaying on top of the VLPs the biofunctional ability of VLPs as a composite macromolecular nanostructure were obtained to target tumors. In order to test this hypothesis VLP-rscFvs associated with LUV-SRB were used here as a test model to deliver to spheroids, a well-studied *ex vivo* tumor model. The second novel aspect of this study is the use of GP64 present on VLPs surface due to silkworm expression system for producing VLPs-rscFv-SRB at neutral pH. Thus efficient expression can be done using silkworm expression system and the purified VLP-rscFvs can be associated with dyes in a simple way facilitated by GP64. In future other known drugs for colon carcinoma can be tried using similar principle.

ACKNOWLEDGMENTS AND DISCLOSURES

We thank Professor Hiroshi Ueda (Tokyo Institute of Technology, Japan) for the kind gift of plasmid carrying ScFv cDNA. This work was supported partly by Grant-in-Aid for Scientific Research (A) Grant No.22248009 and partly by Promotion of Nanobio-Technology Research to support Aging and Welfare Society from the Ministry of Education, Culture, Sports, Science and Technology, Japan. There was no additional external funding received for this study.

REFERENCES

1. Deo VK, Tsuji Y, Yasuda T, Kato T, Sakamoto N, Suzuki H, *et al.* Expression of an RSV-gag virus-like particle in insect cell lines and silkworm larvae. J Virol Methods. 2011;177:147–52.
2. Medina G, Pincetic A, Ehrlich LS, Zhang Y, Tang Y, Leis J, *et al.* Tsg101 can replace Nedd4 function in ASV Gag release but not membrane targeting. Virol. 2008;377:30–8.
3. Waheed AA, Freed EO. The role of lipids in retrovirus replication. Viruses. 2010;2:1146–80.
4. Ma YM, Vogt VM. Rous sarcoma virus Gag protein-oligonucleotide interaction suggests a critical role for protein dimer formation in assembly. J Virol. 2002;76:5452–62.
5. Deo V, Yoshimatsu K, Otsuki T, Dong J, Kato T, Park EY. Display of Neospora caninum surface protein related sequence 2 on Rous sarcoma virus-derived gag protein virus-like particles. J Biotechnol. 2013;165:69–75.
6. Fankhauser N, Maser P. Identification of GPI anchor attachment signals by a Kohonen self-organizing map. Bioinformatics. 2005;21:1846–52.
7. Pierleoni A, Martelli PL, Casadio R. PredGPI: a GPI-anchor predictor. BMC Bioinforma. 2008;9:392–402.
8. Hessa T, Meindl-Beinker NM, Bernsel A, Kim H, Sato Y, Lerch-Bader M, *et al.* Molecular code for transmembrane-helix recognition by the Sec61 translocon. Nature. 2007;450:1026–30.
9. Butikofer P, Malherbe T, Boschung M, Roditi I. GPI-anchored proteins: now you see 'em, now you don't. FASEB J. 2001;15:545–8.
10. Derdak SV, Kueng HJ, Leb VM, Neunkirchner A, Schmetterer KG, Bielek E, *et al.* Direct stimulation of T lymphocytes by immunosomes: virus-like particles decorated with T cell receptor/CD3 ligands plus costimulatory molecules. Proc Natl Acad Sci U S A. 2006;103:13144–9.
11. Dangaj D, Abbott KL, Mookerjee A, Zhao A, Kirby PS, Sandaltzopoulos R, *et al.* Mannose receptor (MR) engagement by mesothelin GPI anchor polarizes tumor-associated macrophages and is blocked by anti-MR human recombinant antibody. PLoS One. 2011;6:28386–99.
12. Wen M, Arora R, Wang H, Liu L, Kimata JT, Zhou P. GPI-anchored single chain Fv-an effective way to capture transiently-exposed neutralization epitopes on HIV-1 envelope spike. Retrovirol. 2010;7:79–96.
13. Chames P, Baty D. Bispecific antibodies for cancer therapy. Curr Opin Drug Discov Devel. 2009;12:276–83.
14. Chames P, Van Regenmortel M, Weiss E, Baty D. Therapeutic antibodies: successes, limitations and hopes for the future. Br J Pharmacol. 2009;157:220–33.
15. Alderson RF, Toki BE, Roberge M, Geng W, Basler J, Chin R, *et al.* Characterization of a CC49-based single-chain fragment-beta-lactamase fusion protein for antibody-directed enzyme prodrug therapy (ADEPT). Bioconjug Chem. 2006;17:410–8.
16. Arruebo M, Vilaboa N, Sáez-Gutierrez B, Lambea J, Tres A, Valladares M, *et al.* Assessment of the evolution of cancer treatment therapies. Cancers. 2011;3:3279–330.
17. Pavlinkova G, Beresford GW, Booth BJ, Batra SK, Colcher D. Pharmacokinetics and biodistribution of engineered single-chain antibody constructs of MAb CC49 in colon carcinoma xenografts. J Nucl Med. 1999;40:1536–46.
18. Iyer U, Kadambi V. Antibody drug conjugates–Trojan horses in the war on cancer. J Pharmacol Toxicol Methods. 2011;64:207–12.

19. Monsma SA, Blissard GW. Identification of a membrane fusion domain and an oligomerization domain in the baculovirus GP64 envelope fusion protein. J Virol. 1995;69:2583–95.
20. Monsma SA, Oomens AG, Blissard GW. The GP64 envelope fusion protein is an essential baculovirus protein required for cell-to-cell transmission of infection. J Virol. 1996;70:4607–16.
21. Oomens AG, Monsma SA, Blissard GW. The baculovirus GP64 envelope fusion protein: synthesis, oligomerization, and processing. Virol. 1995;209:592–603.
22. Li Z, Blissard G. Autographa californica multiple nucleopolyhedrovirus GP64 protein: roles of histidine residues in triggering membrane fusion and fusion pore expansion. J Virol. 2011;85:12492–504.
23. Kamiya K, Tsumoto K, Arakawa S, Shimizu S, Morita I, Yoshimura T, *et al.* Preparation of connexin43-integrated giant liposomes by a baculovirus expression-liposome fusion method. Biotechnol Bioeng. 2010;107:836–43.
24. Tsuji Y, Deo VK, Kato T, Park EY. Production of Rous sarcoma virus-like particles displaying human transmembrane protein in silkworm larvae and its application to ligand-receptor binding assay. J Biotechnol. 2011;155:185–92.
25. Ong SM, Zhao Z, Arooz T, Zhao D, Zhang S, Du T, *et al.* Engineering a scaffold-free 3D tumor model for in vitro drug penetration studies. Biomaterials. 2010;31:1180–90.
26. Jiang X, Sha X, Xin H, Xu X, Gu J, Xia W, *et al.* Integrin-facilitated transcytosis for enhanced penetration of advanced gliomas by poly(trimethylene carbonate)-based nanoparticles encapsulating paclitaxel. Biomaterials. 2013;34:2969–79.
27. Jiang X, Xin H, Gu J, Xu X, Xia W, Chen S, *et al.* Solid tumor penetration by integrin-mediated pegylated poly(trimethylene carbonate) nanoparticles loaded with paclitaxel. Biomaterials. 2013;34:1739–46.
28. Kamiya K, Kobayashi J, Yoshimura T, Tsumoto K. Confocal microscopic observation of fusion between baculovirus budded virus envelopes and single giant unilamellar vesicles. Biochim Biophys Acta. 2010;1798:1625–31.
29. Houghton P, Fang R, Techatanawat I, Steventon G, Hylands P, Lee C. The sulphorhodamine (SRB) assay and other approaches to testing plant extracts and derived compounds for activities related to reputed anticancer activity. Methods (San Diego, Calif). 2007;42:377–87.
30. Sanger F, Nicklen S, Coulson AR. DNA sequencing with chain-terminating inhibitors. Proc Natl Acad Sci U S A. 1977;74:5463–7.
31. Deo VK, Hiyoshi M, Park EY. Construction of hybrib autographa californica nuclear polyhedrosis bacmid by modification of p143 helicase. J Virol Methods. 2006;134:212–6.
32. Maeda T, Ohnishi S. Activation of influenza virus by acidic media causes hemolysis and fusion of erythrocytes. FEBS Lett. 1980;122:283–7.
33. Tamba Y, Yamazaki M. Single giant unilamellar vesicle method reveals effect of antimicrobial peptide magainin 2 on membrane permeability. Biochemistry. 2005;44:15823–33.
34. Bolhassani A, Safaiyan S, Rafati S. Improvement of different vaccine delivery systems for cancer therapy. Mol Cancer. 2011;10:3.
35. Keswani R, Pozdol I, Pack D. Design of hybrid lipid/retroviral-like particle gene delivery vectors. Mol Pharm. 2013;10:1725–35.